Hydrogen bond dynamics in the active site of photoactive yellow protein

Paul A. Sigala, Mark A. Tsuchida, and Daniel Herschlag[1]

Department of Biochemistry, Stanford University, Stanford, CA 94305-5307

Edited by Ann E. McDermott, Columbia University, New York, NY, and approved April 24, 2009 (received for review February 5, 2009)

Hydrogen bonds play major roles in biological structure and function. Nonetheless, hydrogen-bonded protons are not typically observed by X-ray crystallography, and most structural studies provide limited insight into the conformational plasticity of individual hydrogen bonds or the dynamical coupling present within hydrogen bond networks. We report the NMR detection of the hydrogen-bonded protons donated by Tyr-42 and Glu-46 to the chromophore oxygen in the active site of the bacterial photoreceptor, photoactive yellow protein (PYP). We have used the NMR resonances for these hydrogen bonds to probe their conformational properties and ability to rearrange in response to nearby electronic perturbation. The detection of geometric isotope effects transmitted between the Tyr-42 and Glu-46 hydrogen bonds provides strong evidence for robust coupling of their equilibrium conformations. Incorporation of a modified chromophore containing an electron-withdrawing cyano group to delocalize negative charge from the chromophore oxygen, analogous to the electronic rearrangement detected upon photon absorption, results in a lengthening of the Tyr-42 and Glu-46 hydrogen bonds and an attenuated hydrogen bond coupling. The results herein elucidate fundamental properties of hydrogen bonds within the complex environment of a protein interior. Furthermore, the robust conformational coupling and plasticity of hydrogen bonds observed in the PYP active site may facilitate the larger-scale dynamical coupling and signal transduction inherent to the biological function that PYP has evolved to carry out and may provide a model for other coupled dynamic systems.

charge delocalization | hydrogen bond coupling | protein structure | signal transduction

Hydrogen bonds are ubiquitous in nature and central to biological structure and function, including protein and nucleic acid folding, molecular recognition, allostery, signal transduction, and enzymatic catalysis. Networks of adjoining hydrogen bonds frequently form in protein interiors, where they connect secondary structure elements, bridge discrete protein domains, and link together key active site groups. The unique structural and dynamical properties of these networks have been proposed to play fundamental roles to fine-tune protein architecture and position bound ligands, to propagate local conformational changes to remote protein regions, to couple the collective motions of distal groups, and to mediate long-range biological electron transfer (1–6).

Despite the prevalence of hydrogen bonds in biological macromolecules and their extensive characterization in small molecules (7, 8), incisive dissection of specific physical properties that underlie their functional roles within the complex environment of a folded protein remains a formidable challenge. Electron densities for hydrogen-bonded protons are typically not observed in high-resolution X-ray structures. Thus, hydrogen bond formation must be inferred from the proximity of potential donor and acceptor groups. Furthermore, static crystallographic models provide limited information regarding the structural plasticity of individual hydrogen bonds or the dynamical coupling present within hydrogen bond networks.

A critical test case for understanding the intimate interplay between the physical properties of hydrogen bonds and their higher-order functional roles within proteins is provided by the cytosolic bacterial photoreceptor, photoactive yellow protein (PYP). PYP serves as the structural prototype of the Per-Arnt-Sim (PAS) sensory domain and has provided a powerful system to dissect the physical mechanisms of light-activated signal transduction (9–11). Upon absorption of light at 446 nm and rapid charge rearrangement within its thioester-linked *p*-coumaric acid chromophore, PYP initiates a complex photocycle that couples the local *trans-cis* isomerization of a double bond within the chromophore to global conformational restructuring of the protein on the picosecond-to-millisecond time scale (12–14). The phenolic chromophore is stabilized in the photochemical ground state as a phenolate anion by hydrogen bonds donated by Tyr-42 and protonated Glu-46, which form an extended hydrogen bond network within the active site via additional interactions with the side-chain hydroxyl of Thr-50 and backbone amide of Arg-52 (Fig. 1) (15). Disruption of this network via site-directed mutagenesis alters the photoabsorption properties of the chromophore and perturbs the kinetics of several steps within the photocycle (16–18), implying a role for these residues in tuning the ground state photophysics of PYP and the energetics of its conformational transitions during the photocycle. While these mutagenesis studies provide strong evidence for the functional importance of hydrogen bonds, they do not reveal the physical properties of the parent, intact hydrogen bonds that underlie their functional roles during the PYP photocycle.

We report herein the direct detection of the hydrogen-bonded protons donated by Tyr-42 and Glu-46 to the chromophore oxygen in the PYP ground state by solution ^{1}H NMR. We exploit these resonances to incisively address key questions regarding fundamental structural and dynamical properties of these interactions in their intact state and how these properties may change during the earliest events of the photocycle: (*i*) Are conformational rearrangements within one hydrogen bond communicated to the neighboring hydrogen bond? (*ii*) What is the effect of delocalizing charge from the chromophore oxygen, analogous to the electronic redistribution upon photon absorption, on the structures and conformational coupling of these 2 hydrogen bonds?

Results and Discussion

NMR Detection and Assignment of the Tyr-42 and Glu-46 Hydrogen-Bonded Protons. Extensive X-ray crystallographic studies of PYP, including 3 structures determined to better than 1.0 Å resolution (19–21), have revealed 2.5–2.6 Å oxygen-oxygen distances for the hydrogen bonds donated by Tyr-42 and Glu-46 to the chromophore oxygen in the photochemical ground state (Fig. 1). These distances are significantly shorter than those of 2.7–3.1 Å observed for other hydrogen bonds within the protein (20). Short hydrogen bond O···O distances are expected to involve substan-

Author contributions: P.A.S. designed research; P.A.S. and M.A.T. performed research; P.A.S., M.A.T., and D.H. analyzed data; and P.A.S. and D.H. wrote the paper.

The authors declare no conflicts of interest.

This article is a PNAS Direct Submission.

[1]To whom correspondence should be addressed. E-mail: herschla@stanford.edu.

This article contains supporting information online at www.pnas.org/cgi/content/full/0900168106/DCSupplemental.

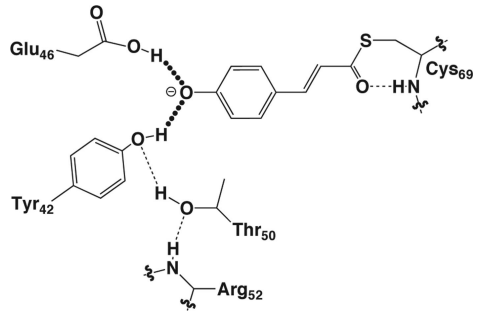

Fig. 1. Schematic depiction of the hydrogen bond network in the PYP active site.

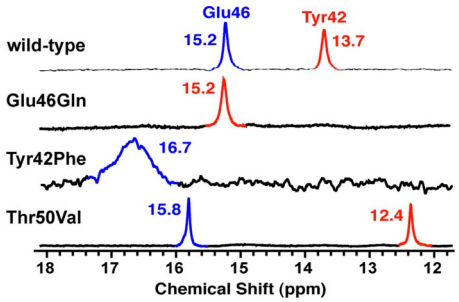

Fig. 2. Downfield region of ^{1}H NMR spectra of wild-type and hydrogen bond mutants of PYP. The broad line-width observed for the Tyr42Phe mutant is consistent with UV/VIS, FT Raman, and fluorescence spectroscopy studies of this mutant that suggested the presence of 2 structurally similar and interconverting chromophore conformations (17). Peaks are color-coded according to their assignment, as explained in the text.

tial lengthening of the donor O-H bond and migration of the bridging proton toward the acceptor oxygen, based on extensive neutron diffraction studies of hydrogen bond structure in small molecules (22, 23). Indeed, elongation of the O-H bond of Glu-46 was observed in a recent 1.5 Å resolution neutron structure of PYP (24). Proton migration decreases sigma bond electron density around the bridging proton and deshields it relative to other protons, resulting in a more downfield NMR chemical shift that correlates with the O···O, O-H, and H···O distances of the hydrogen bond (25, 26).

Consistent with the 2 short O···O distances observed crystallographically for the Tyr-42·chromophore and Glu-46·chromophore hydrogen bonds, we detected 2 far-downfield peaks at 13.7 and 15.2 ppm in the 1-dimensional ^{1}H NMR spectrum of PYP (Fig. 2), in agreement with a previous report (27).* These downfield resonances were not detected in the spectrum of the apo protein lacking the covalently attached chromophore and were shifted upfield upon incorporation of a -CN group to withdraw electron density from the chromophore oxygen, as expected for the protons of Tyr-42 and Glu-46 that are directly hydrogen-bonded to the chromophore oxygen (see below). Furthermore, we observed only 1 downfield peak for each of the Tyr42Phe and Glu46Gln mutants and 2 downfield peaks for the Thr50Val mutant, supporting our peak assignments to Tyr-42 and Glu-46 and ruling out a previous assignment to Thr-50 (Fig. 2 and see below). On the basis of a significantly stronger NOE cross-peak observed in a ^{1}H-^{1}H NOESY spectrum for the 13.7 ppm peak than the 15.2 ppm peak to ring protons of Tyr-42 (Fig. S1), we provisionally assigned the 13.7 ppm peak to Tyr-42 and the 15.2 ppm peak to Glu-46 (Fig. 2). This assignment is strongly supported by additional observations described below, although we note that the central conclusions of our study do not depend on this assignment.

As discussed above, a more downfield chemical shift for a hydrogen-bonded proton correlates with greater proton migration away from the donor oxygen and a shorter donor-acceptor O···O distance in small molecules (26). On the basis of these small-molecule correlations, the chemical shifts of the downfield peaks in PYP may be used to estimate O···O distances of 2.56 and 2.61 Å for the hydrogen bonds donated by Glu-46 and Tyr-42, respectively. A 0.82 Å resolution X-ray structure of PYP (estimated coordinate error ± 0.01 Å) reported a distance of 2.59 Å between the chromophore oxygen and the hydroxyl oxygen of Glu-46 (19), very similar to the NMR-derived distance estimate. However, the O···O distance of 2.48 Å from the crystallographic data for the Tyr-42 hydrogen bond is significantly different from the NMR-derived estimate of 2.61 Å.

*The previous peak assignments were to the Tyr-42 (13.7 ppm) and Thr-50 (15.2 ppm) hydrogen-bonded protons, but an assignment of one of these peaks to the Glu-46 hydrogen-bonded proton could not be ruled out. Our results support assignment of the 13.7 ppm peak to Tyr-42 but strongly suggest that the 15.2 ppm peak arises from Glu-46 and not Thr-50.

An explanation for this paradox is provided by the 2 recent neutron structures of deuterium-exchanged PYP (24, 28). In these structures the hydroxyl deuteron of Tyr-42 refined to a position giving an O-D···O angle of 148° (PDB 2ZOI) and an O-D distance of 0.96 Å (24). In contrast, small-molecule hydrogen bonds with O···O distances of 2.4–2.5 Å typically have O-H···O angles greater than 165° and O-H lengths of 1.1–1.2 Å (22). These observations suggest that the Tyr-42 hydrogen bond has geometric features that deviate from those typically observed in small molecules. These features presumably prevent an accurate O···O distance prediction from the NMR chemical shift of the Tyr-42 hydroxyl proton.

For comparison, the O-H···O angle observed in the neutron structure for the hydrogen bond donated by Glu-46 to the chromophore oxygen is 169° (PDB 2ZOI) and the O-D distance refined to 1.21 Å (24), as expected for small molecules with O···O distances <2.6 Å. The significantly longer hydroxyl O-D bond refined for Glu-46 and more pronounced migration of its bridging deuteron relative to Tyr-42 directly supports our assignment of the more downfield NMR peak to Glu-46 and the more upfield peak to Tyr-42. The geometric deviation of the Tyr-42 hydrogen bond likely results from structural constraints within the folded protein interior on the relative positions of the chromophore and Tyr-42 oxygens, highlighting the ability of packing interactions within macromolecules to alter hydrogen bond properties from those observed in small molecules (29). This deviation would not have been detected without direct observation of the hydrogen-bonded proton by neutron diffraction or NMR.

Direct Detection of Physical Coupling Between the Tyr-42 and Glu-46 Hydrogen Bonds. Perturbation of the Tyr-42 and Glu-46 hydrogen bonds via mutation to Phe and Gln, respectively, resulted in a 1.5 ppm downfield shift in the NMR peak position of the remaining, unperturbed hydrogen-bonded proton (Fig. 2), suggesting increased proton migration toward the chromophore oxygen (see detailed discussion in *SI Text*). Similarly, the Thr50Val mutation, which ablates a hydrogen bond to Tyr-42 and presumably weakens its ability to donate a hydrogen bond to the chromophore (Figs. 1 and 2), resulted in the Tyr-42 peak moving 1.3 ppm upfield and the Glu-46 peak moving 0.6 ppm downfield relative to wild-type PYP. These chemical shift changes are expected for a lengthening of the Tyr-42 hydrogen bond and a concomitant shortening of the Glu-46 hydrogen bond. These results suggest that hydrogen bonds within the active site network of PYP are conformationally coupled, such that a structural perturbation to one is propagated to its connected hydrogen bond neighbors. These changes, however, could have resulted indirectly from additional active site rearrangements accompa-

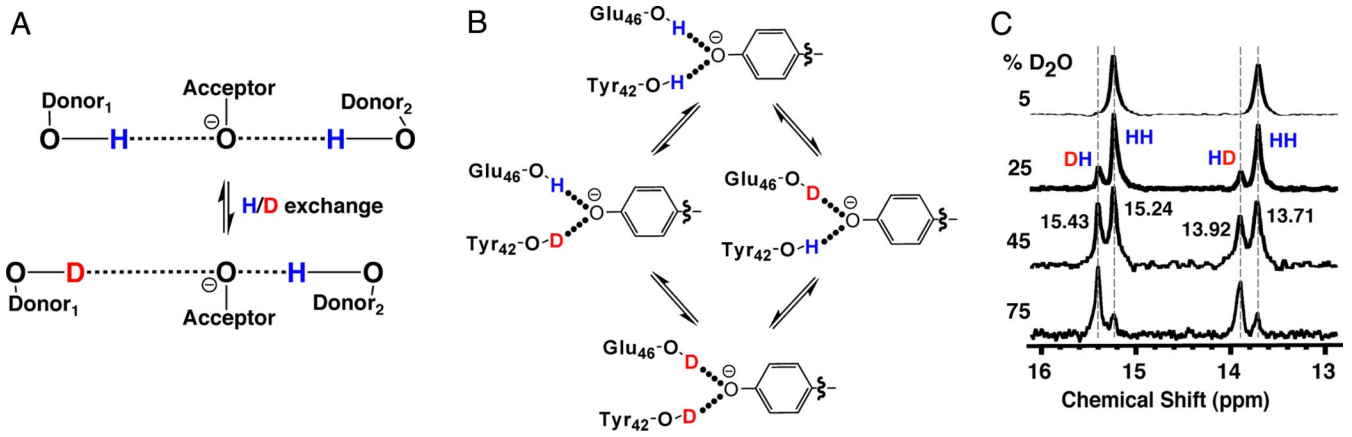

Fig. 3. NMR detection of conformational coupling between the hydrogen bonds donated by Tyr-42 and Glu-46 to the chromophore oxygen. (*A*) Schematic depiction of the conformational changes within a hydrogen bond network upon isotopic substitution. Deuterium substitution of a short hydrogen bond lengthens it by approximately 0.01 Å. This structural rearrangement leads to a shortening of a neighboring hydrogen bond to the same acceptor. (*B*) Hydrogen/deuterium isotopologues of hydrogen bonds in the PYP active site. (*C*) ^{1}H NMR spectra of PYP in solutions containing increasing amounts of D_2O.

nying the mutations. We therefore applied an isotopic substitution method to directly probe physical coupling within the intact hydrogen bond network of PYP.

Hydrogen bonds with O···O distances <2.7 Å are known from small molecule neutron diffraction studies to be particularly susceptible to geometric perturbation upon substitution of the bridging hydrogen by deuterium. Because of anharmonicity in the shape of the hydrogen bond potential energy well, the lower zero-point energy for deuterium results in a shorter O-D bond than the original O-H bond by 0.01–0.02 Å and a lengthening of the O···O distance by a similar magnitude (7, 8, 23, 30). These geometric changes are readily detected by NMR for small molecules in aprotic organic solvents (8, 31, 32).

For a simple network of 2 O-H···O hydrogen bonds to a common acceptor, deuterium substitution of one hydrogen bond has been observed to result in a 0.2–0.3 ppm increase in the chemical shift of the proton in the neighboring hydrogen bond (33, 34). These changes are consistent with a lengthening of the first hydrogen bond by deuteration (due to the shortened O-D covalent bond) and a shortening of the adjacent hydrogen bond in response [shorter hydrogen bonds give rise to increased chemical shifts (26)], as depicted schematically in Fig. 3*A*. The observed transmission of geometric isotope effects through simple hydrogen bond networks within small molecules has provided direct evidence that the conformational properties of adjoining hydrogen bonds are physically coupled. This coupling may derive from subtle modulation of electron density on the acceptor oxygen that occurs upon hydrogen bond lengthening or shortening (7). For example, deuterium substitution of one hydrogen bond and concomitant lengthening of the D···O-acceptor distance may increase electron density on the acceptor oxygen, such that the proton bridging the neighboring hydrogen bond moves toward the acceptor oxygen and the H···O-acceptor distance decreases (Fig. 3*A*).

Are the Tyr-42·chromophore and Glu 46·chromophore hydrogen bonds within the PYP active site conformationally coupled, such that a structural perturbation to one is propagated to the other? Given the short distances of these hydrogen bonds and the detection of their bridging protons via NMR, we hypothesized that the propagation of H/D geometric isotope effects within this network, if present, would be detectable by NMR and thus provide direct evidence for physical coupling between the intact hydrogen bonds. However, it was also possible that larger-scale individual and collective dynamic motions of groups within PYP could swamp out the subtle geometric perturbations introduced by deuterium substitution and hence render any conformational coupling absent or undetectable by NMR. A recent report of geometric isotope effects detected via ^{1}H NMR within a hydrogen bond network in cytosine deaminase indicated that such coupling is indeed detectable in at least one macromolecular system (35).

As the D_2O content of an aqueous solution of PYP increases from 0% to 100%, the protons bridging the Tyr-42 and Glu-46 hydrogen bonds exchange with solvent deuterons to populate the 4 possible hydrogen bond isotopologues depicted in Fig. 3*B*, with the relative populations determined by the isotopic content of the solvent and the H/D fractionation factors of the individual hydrogen bonds (8). While substitution of a proton for a deuteron within either of these hydrogen bonds renders it invisible by ^{1}H NMR, its hydrogen-bonded neighbor remains detectable if its proton has not exchanged with a solvent deuteron (i.e., the 2 central HD isotopologues in Fig. 3*B*). Given the expectation that deuteration of these 2.5–2.6 Å hydrogen bonds will lengthen them by 0.01–0.02 Å (23), propagation of this geometric isotope effect and subsequent shortening of its hydrogen-bonded neighbor would, in principle, be detected as a 0.1–0.3 ppm increase in the chemical shift of its bridging proton, as observed in small molecule studies (33). Thus, if the conformations of the Tyr-42 and Glu-46 hydrogen bonds were indeed coupled in their intact, native states, then we expected to detect a second resonance for each peak as the D_2O content of the solvent increased (4 peaks total), with the newer peaks corresponding to the altered hydrogen bond conformation resulting from deuteration of the neighbor. Alternatively, if the conformations of these hydrogen bonds were not strongly coupled such that the HH and HD isotopologues had equivalent chemical shifts, then we would observe only 2 peaks that decreased in intensity with increasing D_2O content.

At 5% D_2O, we detected only a single peak for each hydrogen-bonded proton, as expected for near-exclusive population of the HH isotopologue. As the deuterium content increased and the HD isotopologues became populated, however, we indeed observed a second, more-downfield peak for each hydrogen-bonded proton (Fig. 3*C*). These new peaks increased in intensity relative to the HH isotopologue peak with increasing solution deuterium content. The NMR data indicate that the chemical shifts and hence equilibrium conformations of the Tyr-42 and Glu-46 hydrogen bonds are altered when the geometry of the adjoining hydrogen bond is perturbed by deuteration, providing direct evidence for physical coupling. Observation of only one downfield peak in 5% and 50% D_2O solutions of the Glu46Gln mutant (Fig. S2), whose longer 2.88 Å Gln·chromophore hydro-

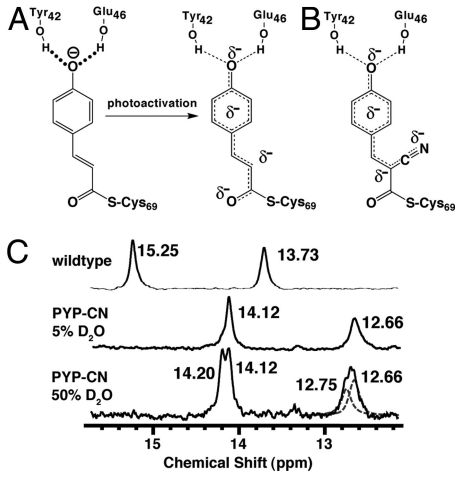

Fig. 4. Probing the effect of charge delocalization from the chromophore oxygen on the structures and coupling of the Tyr-42 and Glu-46 hydrogen bonds. (*A*) Schematic depiction of the charge delocalization from the chromophore oxygen into the extended π-bond network of the ring and substituents in the electronic excited state following photon absorption. (*B*) Incorporation of a modified chromophore containing an electron-withdrawing cyano group mimics the charge delocalization during the PYP electronic excited state. (*C*) ^{1}H NMR spectra of PYP-CN in solutions containing 5% and 50% D_2O. Deconvolution of the 2 overlapping upfield peaks in the 50% D_2O spectrum is shown in gray.

gen bond (20) was not expected to be significantly perturbed upon deuteration, confirmed that changes in hydrogen bond geometry upon deuteration of wild-type PYP are indeed propagated through the intact hydrogen bond network and not due to indirect changes in global protein structure.

For both downfield peaks, the chemical shift of the HD isotopologue is 0.2 ppm more downfield than the HH isotopologue, consistent with increased migration of the bridging proton away from the donor oxygen and shortening of the O···O distance by 0.01 Å. This 0.01 Å change detected in the hydrogen bond retaining its proton is on the same scale as the approximately 0.01 Å lengthening expected for the neighboring hydrogen bond that has been substituted with deuterium, based on small molecule studies of hydrogen bonds with similar lengths (23). Thus, a conformational perturbation to one hydrogen bond is robustly transmitted to its adjoining hydrogen bond neighbor within the PYP active site and is not swamped out by larger-scale individual and collective motions within the protein.

The Effect of Chromophore Charge Delocalization on the Structures and Coupling of the Tyr-42 and Glu-46 Hydrogen Bonds. Absorption of light at 446 nm by the negatively charged chromophore of PYP initiates a complex cycle of conformational changes throughout the protein that span the picosecond-to-millisecond time scale (9, 11). Electronic Stark spectroscopy and ab initio computational studies of PYP have suggested that photon absorption results in an initial electronic excited state in which the negative charge residing on the chromophore oxygen in the ground state is delocalized across the conjugated π-bond system of the chromophore (Fig. 4*A*) (36, 37). These electronic changes lead to formation of intermediates on the picosecond (I_0) and nanosecond (I_1) time scales whose absorption maxima have been red-shifted to 500 and 465 nm, respectively (38, 39). Ultra-high resolution X-ray structures of a cryo-trapped photocycle intermediate formed upon light activation of PYP (0.85 and 1.05 Å), thought to structurally resemble I_1, indicated that the chromophore phenolate remained within hydrogen bonding distances of Tyr-42 and Glu-46 (21, 40), suggesting that these hydrogen bonds are intact in the earlier electronic excited state.

What is the effect of charge delocalization from the chromophore oxygen on the lengths and conformational coupling of the Tyr-42 and Glu-46 hydrogen bonds? While the picosecond lifetime of the PYP electronic excited state precludes direct structural characterization via X-ray diffraction or NMR, ultrafast IR spectroscopy of photoactivated PYP detected a high-energy shift in the side-chain carbonyl stretch frequency of Glu-46 on the time scale of the electronic excited state, suggesting that the Glu-46·chromophore hydrogen bond lengthens in response to charge delocalization (41). Such lengthening was also reported in the cryo-trapped structures of I_1 (21, 40).

To directly assess the impact of chromophore charge rearrangement on the structures and coupling of the Tyr-42 and Glu-46 hydrogen bonds, we reconstituted PYP with a modified chromophore containing an electron-withdrawing cyano group on the double bond, termed PYP-CN (Fig. 4*B*). Incorporation of the -CN group lowers the pK_a of the free chromophore by 1 unit (Fig. S3*A*), as expected for delocalization of negative charge from the phenolate oxygen into the aromatic ring and substituents. This delocalization mimics the analogous charge redistribution within the chromophore upon photoactivation. Consistent with this delocalization, PYP-CN displays an absorbance maximum that is red-shifted 20 nm to 466 nm (Fig. S3*B*). Backbone amide ^{1}H-^{15}N HSQC spectra taken of wild-type PYP and PYP-CN indicated that the global architecture of PYP was minimally perturbed by -CN incorporation, based on the very similar pattern of amide cross-peaks observed for both proteins (Fig. S3*C*).

To assess the effect of chromophore charge delocalization on the lengths of the Tyr-42 and Glu-46 hydrogen bonds, we acquired ^{1}H NMR spectra of PYP-CN. Two downfield peaks were observed, shifted 1.1 ppm upfield relative to their positions in wild-type PYP (Fig. 4*C*). This increase in local magnetic shielding is indicative of subtle rearrangements in the positions of the hydrogen-bonded protons away from the chromophore oxygen and toward the donor oxygens of Tyr-42 and Glu-46. These distance changes are estimated to be 0.06 Å based on the observed chemical shift differences (26). A change in proton position of this magnitude is expected to be accompanied by a lengthening of the hydrogen bond O···O distances by approximately 0.04 Å (22, 42). Thus, lengthening of the Tyr-42 and Glu-46 hydrogen bonds upon charge delocalization from the chromophore oxygen appears to be an intrinsic property of these interactions that will contribute to conformational rearrangements during the PYP photocycle.

We next tested the effect of chromophore charge delocalization and concomitant hydrogen bond lengthening on the conformational coupling of the Tyr-42 and Glu-46 hydrogen bonds by acquiring the NMR spectrum of PYP-CN in 50% D_2O (Fig. 4*C*), as described above for wild-type PYP. We expected deuterium substitution of the longer hydrogen bonds in PYP-CN to result in a smaller perturbation of hydrogen bond length relative to PYP and thus expected to observe a smaller geometric rearrangement in the hydrogen-bonded neighbor than for PYP. Partial deuteration of PYP-CN leads to formation of a second downfield peak for both Tyr-42 and Glu-46, indicating that these hydrogen bonds remain conformationally coupled upon charge delocalization. As expected, the magnitude of the chemical shift difference is smaller, reduced from 0.20 ppm in PYP to 0.09 ppm in PYP-CN, consistent with a smaller perturbation in hydrogen bond length from deuterium substitution and diminished rearrangement of its hydrogen bond neighbor.

It was not possible to probe the lengthening of the Tyr-42 and Glu-46 hydrogen bonds over a broader and systematically varied range of chromophore charge delocalization due to the paucity of modified chromophores containing additional electron-withdrawing groups. To overcome this limitation, we adopted an alternative strategy, as follows. The ionized, thioester-linked *p*-coumaric acid chromophore of PYP is essentially a single ring

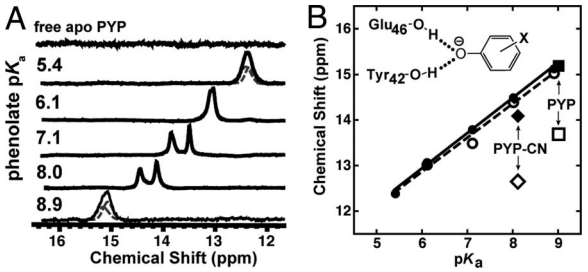

Fig. 5. ^{1}H NMR spectra of apo PYP·phenolate complexes. (*A*) Downfield region of spectra of apo PYP bound to substituted phenolates of increasing pK_a: 3,4-NO_2-phenolate (5.4), 3-F-4-NO_2-phenolate (6.1), 4-NO_2-phenolate (7.1), 4-CN-phenolate (8.0), 4-CF_3-phenolate (8.9). Deconvolution of the 2 overlapping resonances in the highest and lowest pK_a phenolates is shown in gray. (*B*) Correlation between increasing phenolate pK_a and chemical shift of the downfield hydrogen-bonded proton peaks observed in apo PYP·phenolate complexes (circles). Shown for comparison are the chemical shifts of the downfield peaks observed for PYP (squares) and PYP-CN (diamonds), plotted against the phenolate pK_a determined for the respective free chromophore in solution (Fig. S3*A*). The most downfield and second-most downfield peaks are shown as closed and open symbols, respectively.

phenolate substituted in the para position. We hypothesized that a series of free phenols substituted with different electron withdrawing groups in the meta or para positions might bind within the active site cavity of apo PYP as ionized phenolates, accept hydrogen bonds from Tyr-42 and Glu-46, and give rise to detectable downfield NMR peaks. These NMR peaks would then allow us to probe changes in hydrogen bond structure over a broad range of charge delocalization from the phenolate oxygen and, via comparison to native PYP, to test the role of covalent attachment of the phenolate chromophore in tuning the structural properties of the active site hydrogen bonds.

UV absorbance spectra confirmed that apo PYP does indeed bind substituted phenols as ionized phenolates, with a dissociation constant (K_d) of 30 μM observed for 4-nitrophenolate binding (Fig. S4 *A* and *B*). Backbone amide ^{1}H-^{15}N HSQC spectra taken of wild-type PYP and apo PYP saturated with bound 3-F-4-nitrophenolate displayed very similar patterns of amide cross-peaks, suggesting that phenolate-bound apo PYP has a global architecture that is very similar to native, wild-type PYP (Fig. S4*C*).

No downfield peaks with a chemical shift greater than 12 ppm were detected in the ^{1}H NMR spectrum of unliganded apo PYP (Fig. 5*A*). Upon phenolate binding 2 new peaks appeared with chemical shifts greater than 12 ppm, as expected for binding in the active site cavity and formation of hydrogen bonds to Tyr-42 and Glu-46. Active site binding was further supported by the appearance of only 1 downfield peak for phenolate complexes with the Glu46Gln mutant. The 2 downfield peaks had a chemical shift dispersion of 0.3 ppm or less, suggesting nearly identical hydrogen bond lengths. Indeed, for the lowest and highest pK_a phenolates tested, the observed peaks overlapped substantially, requiring line shape simulation to deconvolute the chemical shifts of the individual peaks (Fig. 5*A*). As the pK_a of the bound phenolate decreased from 8.9 to 5.4, delocalizing more negative charge from the phenolate oxygen, the chemical shifts of the observed peaks decreased from 15.1 to 12.4 ppm (Fig. 5 *A* and *B*). This 0.8 ppm chemical shift decrease per unit decrease in pK_a can be used to estimate that the hydrogen bonds donated to the phenolate oxygen lengthen by approximately 0.03 Å upon charge delocalization equivalent to a 1 unit decrease in phenolate pK_a. This lengthening is similar to the lengthening of 0.04 Å per pK_a unit detected between PYP and PYP-CN (Fig. 4*C*).

The chemical shifts of the more downfield peaks observed for PYP and PYP-CN (assigned above to the Glu-46·chromophore hydrogen-bonded proton) fall on the same correlation line as the phenolates (Fig. 5*B*), based on the solution pK_a values of the free chromophores (Fig. S3*A*). However, the more upfield peaks observed for these proteins (assigned to the Tyr-42·chromophore hydrogen-bonded proton) deviate from the behavior of bound phenolates. This deviation, and the substantially nonlinear O-H···O angle of the Tyr-42·chromophore hydrogen bond that appears to underlie it (discussed earlier), presumably reflects the effects of the remainder of the chromophore and its covalent tethering within the active site cavity to constrain the geometry and length of the Tyr-42·chromophore hydrogen bond.

The systematic lengthening of the Tyr-42 and Glu-46 hydrogen bonds upon charge delocalization from the acceptor oxygen closely resembles the behavior of hydrogen bonds donated by Tyr-16 and Asp-103 to phenolates bound in the active site of ketosteroid isomerase, in which we detected an estimated 0.02 Å change in hydrogen bond lengths per change in phenolate pK_a (43). Nevertheless, there are observed differences in the behavior of hydrogen bonds formed to identical phenolates within the 2 distinct protein active sites (Fig. S4*D*), which may arise from differences in the orientations of the hydrogen bond donating groups relative to the oxygen of the bound phenolate or from differential tuning of the relative proton affinities of the donor and acceptor groups via the local electrostatic or geometric environment. These differences highlight the potential of protein active sites to subtly modulate the structural properties of hydrogen bonds on the subangstrom scale (29).

While the limited dispersion of the 2 peaks detected upon phenolate binding prevented investigation of the change in conformational coupling with systematic variation in charge localization via geometric isotope effects, we were able to detect such coupling between the hydrogen-bonded proton peaks in the spectrum of apo PYP bound to 4-nitrophenolate in 50% D_2O (Fig. S4*E*). We expected the chemical shift difference between the HH and HD isotopologues of bound 4-nitrophenolate to be smaller than observed for either PYP or PYP-CN, based on its more upfield NMR peaks and presumably longer hydrogen bonds relative to PYP or PYP-CN (Fig. 5*B*). However, the observed 0.15 ppm chemical shift difference was intermediate between that detected for PYP (0.20 ppm) and PYP-CN (0.09 ppm), providing further evidence for the role of covalent attachment or binding interactions with the remainder of the chromophore in tuning hydrogen bond properties.

Implications. Knowledge of the dynamical motions of groups within proteins spanning a hierarchy of distance and time scales is rapidly increasing (44, 45). Such dynamic behavior appears to be an intrinsic property of biomolecules and may play an important role in biological function. While dynamical motions are increasingly possible to detect, assessing whether such motions are coupled remains a formidable challenge.

The results herein illuminate fundamental conformational properties of hydrogen bonds within the complex environment of a protein interior and help elucidate the potential role of coupled motions within hydrogen bond networks. We have provided direct evidence of conformational coupling for 2 adjoining hydrogen bonds in the active site of PYP. While the magnitude of distance changes attendant to H/D geometric isotope effects are subtle and no larger than 0.01–0.02 Å, the strong coupling between the primary and propagated distance changes introduced by deuterium substitution suggests that larger transmitted effects are possible for larger initial perturbations. Thus, larger conformational changes to hydrogen bonds on the scale of 0.1 Å or greater may be robustly transmitted to adjoining hydrogen bonds. Indeed, the structural rearrangements we observed in response to mutations within the PYP hydrogen bond network support this view (Fig. 2). Conformational coupling within networks of adjoining hydrogen bonds

may therefore facilitate the transmission of structural rearrangements across significant distances and thus promote larger-scale dynamical coupling and signal transduction within proteins, as proposed in several systems (2–4). Hydrogen bond coupling may be particularly crucial for modulating the proximity of donor and acceptor groups within proteins catalyzing proton-coupled electron transfer, due to the exquisite sensitivity of electron transfer efficiency to the donor-acceptor distance (5, 6, 46).

While the structural rearrangements upon charge delocalization we have detected via solution NMR within the network of hydrogen bonds donated by Tyr-42 and Glu-46 to the chromophore oxygen of PYP reflect changes that have equilibrated with the surrounding protein matrix, they suggest that analogous nonequilibrium hydrogen bond rearrangements may accompany the earliest events of the PYP photocycle following photon absorption. Thus, we propose that charge delocalization from the chromophore oxygen upon photoactivation leads to lengthening and attenuated coupling of the Tyr-42 and Glu-46 hydrogen bonds. These changes and their propagated effects through the extended hydrogen bond network leading to Arg-52 may promote the subsequent structural reorganizations during the photocycle, including movement of the Arg-52 side-chain and flipping of the chromophore ring out of the active site pocket in I_2 (47, 48).

Methods

PYP was expressed and purified from *E. coli* and reconstituted with the wild-type or cyanylated *p*-coumaric acid chromophore (Sigma-Aldrich) using previously reported methods (16) with minor modifications. 1D ^{1}H, 2D ^{1}H-^{1}H NOESY, and 2D ^{1}H-^{15}N HSQC spectra were acquired using previously reported methods (29, 43). Hydrogen bond distances were estimated from NMR chemical shifts using published correlations that relate the measured chemical shift of the hydrogen-bonded proton to the O···O or H···O-acceptor distances (26, 42). Spectral deconvolutions were carried out using the ACD/NMR Processor software. A full description of experimental methods is given in *SI Text*.

ACKNOWLEDGMENTS. We thank E. Getzoff for providing plasmids encoding PYP; C. Liu and S. Lynch for assistance with NMR experiments; S. Anderson, S. Boxer, J. Brauman, A. Fafarman, P. Harbury, C. Khosla, J. Klinman, H. Limbach, K. Moffat, and P. Tolstoy for helpful discussions; and members of the Herschlag laboratory for comments on the manuscript. This work was funded by a National Science Foundation grant to D.H. (MCB-0641393). P.A.S. was supported in part by Howard Hughes Medical Institute and Lieberman Predoctoral Fellowships. M.A.T. was supported in part by a National Institutes of Health Cellular and Molecular Biology Training Grant.

1. Fersht AR (1999) *Structure and Mechanism in Protein Science* (W.H. Freeman and Company, New York).
2. Rodriguez JC, Zeng YH, Wilks A, Rivera M (2007) The hydrogen-bonding network in heme oxygenase also functions as a modulator of enzyme dynamics: Chaotic motions upon disrupting the H-bond network in heme oxygenase from *Pseudomonas aeruginosa*. *J Am Chem Soc* 129:11730–11742.
3. Bouvignies G, et al. (2005) Identification of slow correlated motions in proteins using residual dipolar and hydrogen-bond scalar couplings. *Proc Natl Acad Sci USA* 102:13885–13890.
4. Peralvarez-Marin A, et al. (2007) Inter-helical hydrogen bonds are essential elements for intra-protein signal transduction: The role of Asp115 in bacteriorhodopsin transport function. *J Mol Biol* 368:666–676.
5. Derege PJF, Williams SA, Therien MJ (1995) Direct evaluation of electronic coupling mediated by hydrogen-bonds: Implications for biological electron-transfer. *Science* 269:1409–1413.
6. Reece SY, Hodgkiss JM, Stubbe J, Nocera DG (2006) Proton-coupled electron transfer: The mechanistic underpinning for radical transport and catalysis in biology. *Philos Trans Royal Soc B* 361:1351–1364.
7. Jeffrey GA (1997) *An Introduction to Hydrogen Bonding* (Oxford Univ Press, New York).
8. Hibbert F, Emsley J (1990) Hydrogen bonding and chemical reactivity. *Adv Phys Org Chem* 26:255–379.
9. Cusanovich MA, Meyer TE (2003) Photoactive yellow protein: A prototypic PAS domain sensory protein and development of a common signaling mechanism. *Biochemistry* 42:4759–4770.
10. Pellequer JL, Wager-Smith KA, Kay SA, Getzoff ED (1998) Photoactive yellow protein: A structural prototype for the three-dimensional fold of the PAS domain superfamily. *Proc Natl Acad Sci USA* 95:5884–5890.
11. Hellingwerf KJ, Hendriks J, Gensch T (2003) Photoactive yellow protein, a new type of photoreceptor protein: Will this ''yellow lab'' bring us where we want to go? *J Phys Chem A* 107:1082–1094.
12. Rubinstenn G, et al. (1998) Structural and dynamic changes of photoactive yellow protein during its photocycle in solution. *Nat Struct Biol* 5:568–570.
13. Hoff WD, et al. (1999) Global conformational changes upon receptor stimulation in photoactive yellow protein. *Biochemistry* 38:1009–1017.
14. Brudler R, et al. (2006) PAS domain allostery and light-induced conformational changes in photoactive yellow protein upon I2 intermediate formation, probed with enhanced hydrogen/deuterium exchange mass spectrometry. *J Mol Biol* 363:148–160.
15. Borgstahl GE, Williams DR, Getzoff ED (1995) 1.4 Å structure of photoactive yellow protein, a cytosolic photoreceptor: unusual fold, active site, and chromophore. *Biochemistry* 34:6278–6287.
16. Genick UK, et al. (1997) Active site mutants implicate key residues for control of color and light cycle kinetics of photoactive yellow protein. *Biochemistry* 36:8–14.
17. Brudler R, et al. (2000) Coupling of hydrogen bonding to chromophore conformation and function in photoactive yellow protein. *Biochemistry* 39:13478–13486.
18. Philip AF, Eisenman KT, Papadantonakis GA, Hoff WD (2008) Functional tuning of photoactive yellow protein by active site residue 46. *Biochemistry* 47:13800–13810.
19. Getzoff ED, Gutwin KN, Genick UK (2003) Anticipatory active-site motions and chromophore distortion prime photoreceptor PYP for light activation. *Nat Struct Biol* 10:663–668.
20. Anderson S, Crosson S, Moffat K (2004) Short hydrogen bonds in photoactive yellow protein. *Acta Crystallogr D* 60:1008–1016.
21. Genick UK, Soltis SM, Kuhn P, Canestrelli IL, Getzoff ED (1998) Structure at 0.85 Å resolution of an early protein photocycle intermediate. *Nature* 392:206–209.
22. Steiner T, Saenger W (1994) Lengthening of the covalent O-H bond in O-H—O hydrogen bonds re-examined from low-temperature neutron diffraction data of organic compounds. *Acta Crystallogr B* 50:348–357.
23. Ichikawa M (2000) Hydrogen-bond geometry and its isotope effect in crystals with OHO bonds—revisited. *J Mol Struct* 552:63–70.
24. Yamaguchi S, et al. (2009) Low-barrier hydrogen bond in photoactive yellow protein. *Proc Natl Acad Sci USA* 106:440–444.
25. Rohlfing CM, Allen LC, Ditchfield R (1983) Proton chemical-shift tensors in hydrogen-bonded dimers of rcooh and roh. *J Chem Phys* 79:4958–4966.
26. Jeffrey GA, Yeon Y (1986) The correlation between hydrogen-bond lengths and proton chemical shifts in crystals. *Acta Crystallogr B* 42:410–413.
27. Dux P, et al. (1998) Solution structure and backbone dynamics of the photoactive yellow protein. *Biochemistry* 37:12689–12699.
28. Fisher SZ, et al. (2007) Neutron and X-ray structural studies of short hydrogen bonds in photoactive yellow protein (PYP). *Acta Crystallogr D* 63:1178–1184.
29. Sigala PA, et al. (2008) Testing geometrical discrimination within an enzyme active site: Constrained hydrogen bonding in the ketosteroid isomerase oxyanion hole. *J Am Chem Soc* 130:13696–13708.
30. Ubbelohde AR, Gallagher KJ (1955) Acid-base effects in hydrogen bonds in crystals. *Acta Crystallogr* 8:71–83.
31. Altman LJ, Laungani D, Gunnarsson G, Wennerstrom H, Forsen S (1978) Proton, deuterium, and tritium nuclear magnetic resonance of intramolecular hydrogen bonds. Isotope effects and the shape of the potential energy function. *J Am Chem Soc* 100:8264–8266.
32. Smirnov SN, et al. (1996) Hydrogen deuterium isotope effects on the NMR chemical shifts and geometries of intermolecular low-barrier hydrogen-bonded complexes. *J Am Chem Soc* 118:4094–4101.
33. Tolstoy PM, et al. (2004) Characterization of fluxional hydrogen-bonded complexes of acetic acid and acetate by NMR: geometries and isotope and solvent effects. *J Am Chem Soc* 126:5621–5634.
34. Bolvig S, Hansen PE (2000) Isotope effects on chemical shifts as an analytical tool in structural studies of intramolecular hydrogen bonded compounds. *Curr Org Chem* 4:19–54.
35. Liu A, et al. (2008) NMR detection of bifurcated hydrogen bonds in large proteins. *J Am Chem Soc* 130:2428–2429.
36. Premvardhan LL, van der Horst MA, Hellingwerf KJ, van Grondelle R (2003) Stark spectroscopy on photoactive yellow protein, E46Q, and a nonisomerizing derivative, probes photo-induced charge motion. *Biophys J* 84:3226–3239.
37. Molina V, Merchan M (2001) On the absorbance changes in the photocycle of the photoactive yellow protein: A quantum-chemical analysis. *Proc Natl Acad Sci USA* 98:4299–4304.
38. Meyer TE, Yakali E, Cusanovich MA, Tollin G (1987) Properties of a water-soluble, yellow protein isolated from a halophilic phototrophic bacterium that has photochemical activity analogous to sensory rhodopsin. *Biochemistry* 26:418–423.
39. Ujj L, et al. (1998) New photocycle intermediates in the photoactive yellow protein from *Ectothiorhodospira halophila*: Picosecond transient absorption spectroscopy. *Biophys J* 75:406–412.
40. Anderson S, Srajer V, Moffat K (2004) Structural heterogeneity of cryotrapped intermediates in the bacterial blue light photoreceptor, photoactive yellow protein. *Photochem Photobiol* 80:7–14.
41. Groot ML, et al. (2003) Initial steps of signal generation in photoactive yellow protein revealed with femtosecond mid-infrared spectroscopy. *Biochemistry* 42:10054–10059.
42. Harris TK, Mildvan AS (1999) High-precision measurement of hydrogen bond lengths in proteins by nuclear magnetic resonance methods. *Proteins* 35:275–282.
43. Kraut DA, et al. (2006) Testing electrostatic complementarity in enzyme catalysis: hydrogen bonding in the ketosteroid isomerase oxyanion hole. *PLoS Biol* 4:e99.
44. Karplus M, Kuriyan J (2005) Molecular dynamics and protein function. *Proc Natl Acad Sci USA* 102:6679–6685.
45. Boehr DD, Dyson HJ, Wright PE (2006) An NMR perspective on enzyme dynamics. *Chem Rev* 106:3055–3079.
46. Hatcher E, Soudackov AV, Hammes-Schiffer S (2004) Proton-coupled electron transfer in soybean lipoxygenase. *J Am Chem Soc* 126:5763–5775.
47. Genick UK, et al. (1997) Structure of a protein photocycle intermediate by millisecond time-resolved crystallography. *Science* 275:1471–1475.
48. Rajagopal S, et al. (2005) A structural pathway for signaling in the E46Q mutant of photoactive yellow protein. *Structure* 13:55–63.